Published in final edited form as:
Langmuir. 2011 September 6; 27(17): 10412–10420. doi:10.1021/la2013705.

Formulation and Acoustic Studies of a New Phase-Shift Agent for Diagnostic and Therapeutic Ultrasound

Paul S. Sheeran[1], **Samantha Luois**[2,3], **Paul A. Dayton**[1], and **Terry O. Matsunaga**[2,*]

[1]Joint Dept. of Biomedical Engineering, University of North Carolina and NC State University, Chapel Hill, North Carolina

[2]Dept. of Radiology Research, University of Arizona, Tucson, Arizona

[3]Undergraduate Biology Research Program, University of Arizona, Tucson, Arizona

Abstract

Recent efforts in the area of acoustic droplet vaporization with the objective of designing extravascular ultrasound contrast agents has led to the development of stabilized, lipid-encapsulated nanodroplets of the highly volatile compound decafluorobutane (DFB). We have developed two methods of generating DFB droplets, the first of which involves condensing DFB gas (boiling point of −1.1° to −2° C) followed by extrusion with a lipid formulation in HEPES buffer. Acoustic droplet vaporization of micron-sized lipid-coated droplets at diagnostic ultrasound frequencies and mechanical indices were confirmed optically. In our second formulation methodology, we demonstrate the formulation of sub-micron sized lipid-coated nanodroplets based upon condensation of pre-formed microbubbles containing DFB. The droplets are routinely in the 200 – 300 nm range and yield microbubbles on the order of 1 – 5 microns once vaporized, consistent with ideal gas law expansion predictions. The simple and effective nature of this methodology allows for the development of a variety of different formulations that can be used for imaging, drug and gene delivery, and therapy. This study is the first to our knowledge to demonstrate both a method of generating ADV agents by microbubble condensation and formulation of primarily sub-micron droplets of decafluorobutane that remain stable at physiological temperatures. Finally, activation of DFB nanodroplets is demonstrated using pressures within the FDA guidelines for diagnostic imaging, which may minimize the potential for bioeffects in humans. This methodology offers a new means of developing extravascular contrast agents for diagnostic and therapeutic applications.

Keywords

ultrasound contrast agent; acoustic droplet vaporization; perfluorocarbon; microbubble; nanodroplet; pressurization; condensation

Introduction

Microbubbles for diagnostic ultrasound imaging have been established in the clinical arena as a sensitive and inexpensive imaging technique for interrogating landmarks in the

tmatsunaga@radiology.arizona.edu.

Supporting Information.

Videos of both extruded decafluorobutane microdroplet vaporization and microbubble-condensed sub-micron droplet vaporization under the influence of 5 MHz ultrasound are provided. This information is available free of charge via the Internet at http://pubs.acs.org/.

vasculature. Currently, microbubble-enhanced diagnostic ultrasound has been approved by the FDA for the study of wall motion abnormalities and ventricular contraction in echocardiography.[1] Researchers have proposed microbubble-aided ultrasound for a wide range of potential applications, including functional tumor, kidney, and liver imaging, identification of vascular inflammation and vulnerable plaque deposition, thrombus detection, and targeted molecular imaging of angiogenesis.[2–6] In addition to the aforementioned studies, microbubbles have been used for therapeutic interventions; primarily in concert with ultrasound-mediated cavitation for sonothrombolysis.

Despite their utility as vascular contrast agents and potential for therapeutic applications, microbubble size (typically 1 – 5 microns in diameter) prevents their transport outside of the vasculature - commonly referred to as extravasation. The exact size limit for nanoparticle extravasation into the interstitial space in solid tumors depends on a variety of factors, but usually falls within the range of 100 nm – 750 nm.[7] Bubbles small enough to diffuse past these inter-endothelial gap junctions would scatter ultrasound energy poorly compared to typical microbubbles, and would provide limited imaging contrast.[8] Additionally, microbubble circulation *in vivo* is shown to be on the order of tens of minutes before bubble dissolution and clearance significantly limits contrast enhancement.[9,10] This short time period may be insufficient for enough bubbles to accumulate by diffusion into the tumor interstitium.

Recently there has been interest in the concept of ultrasound-mediated vaporization of perfluorocarbon (PFC) droplets for the purposes of vascular occlusion, ultrasound-mediated tissue ablation, and contrast enhancement of the tumor interstitium combined with drug delivery.[11–14] The phenomenon by which droplets undergo a phase-shift as a result of acoustic pressure is most commonly noted in the literature as *acoustic droplet vaporization* (ADV).[15,16] Many *in vitro* studies have shown that the acoustic output necessary to induce vaporization increases as a function of decreased diameter, decreased frequency, and increased perfluorocarbon boiling point.[13,17,18] While preliminary *in vivo* studies have been promising[11,14,19], applications involving relatively low frequencies and/or sub-micron droplets may require pressures higher than diagnostic ultrasound machines currently provide[12], increasing the potential for unwanted bioeffects. Thus, a nanometer-scale droplet or nanodroplet that is more susceptible to ultrasound pressures yet stable at physiological temperatures could provide a more efficacious vehicle for extravasation into tissue and activation at the site of action in many applications. The main objective of this study was to develop stable sub-micron droplets capable of being vaporized using frequencies and mechanical indices within the FDA-approved limits of commercial clinical diagnostic ultrasound machines.

Work by others involving nanodroplets capable of diffusing past the vascular endothelial membrane in solid tumors for the purpose of ADV or as liquid ultrasound scatterers have typically utilized perfluorocarbons with boiling points above room temperature (25° C), and have relied on extrusion or emulsification to generate droplets.[12,14,20–22] Initial studies in the laboratory of Rapoport and coworkers[14] used the Antoine vapor pressure equation[23] to assess the theoretical vaporization temperature dependence upon droplet diameter of selected perfluorocarbons as a result of the influence of interfacial surface tension. They concluded that the temperatures required to vaporize smaller droplets increased geometrically as droplet size decreased into the submicron range. Extending this model to investigate the influence of perfluorocarbon boiling points reveals that less volatile PFC compounds such as dodecafluoropentane, perfluorohexane, perfluoroheptane, etc., may require a relatively large amount of energy in order to elicit droplet vaporization at a size that would practically be able to extravasate through endothelial gap junctions into the extravascular space (see Figure 1). Assuming a correlation between the temperature increase

over body temperature needed to vaporize and ultrasound energies, the lower boiling PFCs, such as decafluorobutane (DFB) and octafluoropropane, may be more attractive for certain applications since the acoustic energy required to induce ADV would be significantly less. This issue becomes especially important when designing an agent for extravascular diagnostic ultrasound imaging, as high acoustic energies may result in unwanted bioeffects.

However, the utilization of perfluorobutane (boiling point of −1.1° to −2° C)[26] and other compounds with boiling points far below physiological and room temperatures can make stabilized droplet formulation somewhat challenging. Nonetheless, should these PFCs be successfully condensed and stabilized, their utility as ultrasound-mediated bubble precursors for extravascular applications would expand the possibilities of diagnostic ultrasound imaging and drug delivery. Recent efforts in our laboratories have indicated that this indeed may be the case.[27]

An ideal extravascular ultrasound contrast agent for applications where thermal and cavitation-based bioeffects are minimized should be: 1) stable in the vasculature for a sufficient time period: 2) capable of extravasation out of the vascular space, and: 3) labile enough to be activated and interrogated by clinical ultrasound machines at clinically relevant acoustic intensities. This manuscript details our recent work to develop decafluorobutane nanodroplets with the aforementioned characteristics in mind.

We report two methods to formulate decafluorobutane nanodroplets. The first methodology involves condensing and extruding a lipid and DFB formulation at a temperature below the boiling point of DFB, as reported previously.[27] The second methodology involves a simple process of first generating lipid-coated microbubbles through standard agitation-based techniques[28] followed by ambient air pressurization and slow cooling to condense the gas core of the microbubbles, resulting in sub-micron liquid droplets. The latter methodology offers the advantage of making smaller, more uniform droplet sizes with peaks on the order of 200 – 300 nm - small enough for potential extravasation into solid tumors. Vaporization of the droplets generated from both techniques is performed at acoustic energy parameters compatible with clinical diagnostic ultrasound machines. In this latter method, which we refer to as ‘nanodroplet generation via microbubble condensation’, we have developed a simple, resource-efficient method to create droplets predominantly in the sub-micron range consisting of DFB in an encapsulating shell. When exposed *in vitro* to a 2 μs ultrasound pulse at 5 MHz and MI = 1.2, the generated nanodroplets yield a distribution of microbubbles that corresponds well with expected expansion of the initial droplets through ideal gas law predictions with surface tension effects included[27,29]. These results indicate the potential usefulness of decafluorobutane nanodroplets as a potential ultrasound contrast agent for extravascular imaging.

Materials and Methods

Decafluorobutane Droplet Formulation via Extrusion

Lipid thin films were prepared with a composition containing 85 mole percent dipalmitoylphosphatidylcholine (DPPC), 10 mole percent 1-palmitoyl-2-hydroxy-***sn***-glycero-3-phosphocholine (LPC), and 5 mole percent 1,2-dipalmitoyl-***sn***-glycero-3-phosphoethanolamine-N-[methoxy(polyethylene glycol)-2000] (DPPE-PEG- 2000) (Avanti Polar Lipids, Alabaster, Ala). The lipids were first dissolved in chloroform (EMD Chemicals, Brookfield, WI) and dried over nitrogen gas, then further dried *in vacuo* overnight to remove residual solvent from the lipid films. Approximately 1 mL of HEPES (4-(2-hydroxyethyl)piperazine-1-ethanesulfonic acid) buffer (pH = 7.4) was used to rehydrate the films, which were then sonicated for 10 minutes in a water bath sonicator (Branson 1510, Danbury, CT) at 50 – 60° C. The rehydrated films were subjected to 10

freeze-thaw cycles using an isopropanol bath with dry ice and thawing with a 50 – 60° C water bath, followed by 10 minutes of stirring at 50 – 60° C. This created a lipid suspension which was immediately stirred for 10 minutes at 50–60 °C. The resulting 20 mg/mL lipid suspension was mixed with glycerol (20%, v:v) just prior to performing the extrusion.

Decafluorobutane (FluoroMed, Round Rock, TX) was condensed in a Secure™ EVA Container (Metrix Co., Dubuque, IA) over dry ice. The condensed DFB was poured into a 2 mL glass vial, crimped, and stored at −20° C to preserve the liquid state. The lipid solution (1.5 mL) was brought into the −20° C cold room and allowed to cool to approximately −2° to −5° C, after which 200 μL of DFB was mixed with the lipid solution. The samples were extruded by 20 passes through a 1 μm porous membrane filter (Whatman Ltd., Piscataway, NJ) while the lipid solution was near −5° C to avoid freezing of the aqueous solution and maintain the liquid state of the DFB. After extrusion, the resulting emulsion was stored at 4° C in a crimped 2 mL vial with room air in the headspace. Samples were observed throughout the extrusion process to make sure they did not freeze.

Nanodroplet Formulation via Microbubble Condensation using Room Air

Decafluorobutane microbubbles were formulated by the dissolution of 1,2-dipalmitoyl-sn-glycero 3-phosphatidylcholine (DPPC), 1,2-dipalmitoyl-sn-glycero-3-phosphatidylethanolamine-polyethyleneglycol-2000 (DPPE-PEG-2000), and 1,2-dipalmitoyl-3-trimethylammonium propane (chloride salt; 16:0 TAP) in a molar ratio of 65:5:30 and a total lipid concentration of 0.75 mg/mL, 1.5 mg/mL, and 3 mg/mL. The excipient liquid was comprised of propylene glycol, glycerol, and normal saline (15:5:80). After adding 1.5 mL of the resulting solution to a 2 mL vial, microbubbles were formed via agitation using a Vialmix™ shaker (Bristol-Myers-Squibb, New York, NY) for 45 seconds. The 2 mL vial containing the formed microbubbles was then immersed in a CO_2/isopropanol bath controlled to a temperature of approximately −5° C. A 25 G syringe needle containing 30 mL of room air was then inserted into the vial septum and the plunger depressed slowly until the headspace of the vial was pressurized to between 600 – 750 kPa (approximately 85–110 psi). Lipid freezing was avoided by observing the contents of the vial as well as the temperature of the CO_2/isopropanol solution periodically. The syringe needle was removed from the vial after pressurizing, leaving a pressure head on the solution.

Sample Sizing

Samples prepared by each method were tested in the nanometer range using a Malvern Nano ZS (Malvern Instruments Ltd., Malvern, Worcestershire, UK) and in the micrometer range using an Accusizer 780A (Particle Sizing Systems, Santa Barbara, CA) for distribution statistics. For Accusizer samples, volumes were typically 3 μL for bubbles produced by agitation and 25–50 μL for droplets. Nano ZS sample volumes of 150 – 300 μL diluted in 1 mL of HEPES buffer (pH = 7.4) were used for extruded liquid DFB droplets and 1 mL (undiluted) for room-air microbubble-condensed nanodroplets and lipid solution controls. The upper sizing sensitivity on the Nano ZS was 6 μm in diameter, while the lower sizing sensitivity on the Accusizer 780A was 0.54 μm in diameter, such that an accurate representation of the content over a wide range of sizes could be obtained.

Acoustic Vaporization of Extruded Liquid Decafluorobutane Droplets and Microbubble Condensation Nanodroplets

Experimental Apparatus—The setup used for these experiments was identical to that described in earlier studies.[27] Briefly, an inverted microscope (Olympus IX71, Center Valley, PA) with a water bath passively heated to 37 °C mounted on top was interfaced with a high-speed camera (FastCam SA1.1, Photron USA, Inc., San Diego, CA) to capture images through a 100X NA=1.0 water immersion objective. The optical resolution of the

system was measured to be approximately 0.5 μm, although only droplets and bubbles larger than 1 μm could be measured with reasonable accuracy. For experiments involving degassed water, an in-line degasser was allowed to operate for 30 minutes prior to the experiment and turned off briefly during the vaporization to minimize the vibration present in the captured images. Baseline oxygen saturation at 37 °C was measured to be approximately 5 PPM (Oxygen CHEMets, CHEMetrics, Inc., Calverton, VA), which dropped to 1.5 PPM or less after 30 minutes of degassing. The droplet solution was pumped through a nearly optically and acoustically transparent cellulose tube with a 200 μm inner diameter (Spectrum Labs, Inc., Greensboro, NC). A 3-axis micropositioner (MMO-203, Narishige Group, East Meadow, NY) was used to position the cellulose tube and keep the droplets/bubbles in the field of view, while a custom-built manual injector allowed for precise administration of the droplets into the field of view.

A spherically focused 5 MHz transducer with a focal length of 3.81 cm. (IL0506HP, Valpey Fisher Corp., Hopkinton, MA) was used to insonify droplet samples with signals constructed using an arbitrary waveform generator (AWG 2021, Tektronix, Inc., Beaverton, Or). A synchronization pulse from the waveform generator was relayed to the high speed camera in order to trigger a marker with the acoustic pulse on the digital video. The waveform from the generator, consisting of a 10-cycle sinusoid of adjustable amplitude at 5 MHz (total insonification time of 2 μs), was amplified approximately 60 dB using an RF amplifier (A500, ENI, Rochester, NY) in order to excite the transducer. For optical-acoustic alignment, the transducer focus was matched with the optical focus by a needle hydrophone (HNA-0400, Onda Corp., Sunnyvale, CA). The transducer was calibrated at the focus over the range of amplitudes used to determine the pressure exerted on the droplets in the field of view.

Analysis of images—Still images and videos were captured using proprietary camera software (PFV, Photron USA, Inc., San Diego, CA). Image analyses were performed on the recordings using ImageJ software (NIH, Bethesda).

Vaporization Threshold of Individual Micron-sized Droplets of Extruded Liquid Decafluorobutane—The vaporization threshold of individual PFB droplets was determined by first venting the undiluted samples with a 20-gauge needle and then diluting in degassed (3 PPM oxygen saturation) phosphate-buffered saline (PBS) until only 1 – 2 droplets were visible on screen at any particular time. This typically ranged from 0.1% –2% sample in PBS (v:v) and depended on the concentration of larger droplets present in the original sample. The droplets were held on screen with the position manipulator and ultrasound pressure was increased in steps of approximately 0.115 MPa with 1 – 2 seconds of rest time between e ach trigger. The pressure that induced observed vaporization was recorded to correlate to droplet diameter with ADV acoustic properties.

For analysis, the pressure that induced vaporization was converted to Mechanical Index (MI), defined as:

$$\frac{\text{Peak Negative Pressure (MPa)}}{\sqrt{\text{US Frequency (MHz)}}}$$

Vaporization Threshold of Decafluorobutane Microbubble Condensation Nanodroplets—Due to the fact that droplets smaller than 1 μm were beyond the resolution capabilities of the experimental setup, the approach to vaporize sub-micron droplet samples differed from the individual droplet approach previously described. Samples were left undiluted to maximize the number of droplets and resulting bubbles in the field of

view. Oxygenation after microbubble condensation was typically on the order of 2–3 PPM. Once injected into the *in vitro* setup, the sub-micron droplet samples at each lipid concentration (0.75, 1.5, and 3.0 mg/mL) were exposed to 5 MHz ultrasound pulses 2 μs in duration at a mechanical index of either 1.2 or 1.7. These mechanical indices were chosen because they represent pressures at the middle-to-higher end of what is available on a diagnostic ultrasound machine. Videos of droplet vaporization were taken at the 'mid-plane' of the cellulose tube to observe bubbles as they floated past the focus, and at the top of the tube to observe the bubbles accumulating due to buoyancy. Bubbles were counted and measured to determine any differences in size distributions and/or quantity based on lipid concentration. The size distributions of bubbles obtained at each mechanical index were compared to determine the impact of the pressure level on the resulting size distribution.

Results and Discussion

Acoustic Droplet Vaporization of Decafluorobutane Formulations made via Extrusion

Liquid decafluorobutane extrusions, when sized by the Malvern and Accusizer, yielded content in both the sub-micron and micron size range. Upon exposure to ultrasonic energy, vaporization of the largest content present in the samples – droplets larger than 1 μm, which could be resolved optically - was achieved at clinically relevant pressures such that an inverse relationship between initial diameter and pressure required to vaporize could be observed (Figure 2). Even when left un-diluted and exposed to high mechanical indices, samples produced by this method did not yield a significant amount of bubbles in the 1–5 μm range, suggesting that the sub-micron droplets were either: 1) a small portion of the total sample: 2) unviable: 3) aggregated: 4) required higher acoustic pressures than currently used (the highest pressure used was MI = 2.25), or: 5) a combination of these. Micron-sized droplets were observed to be as large as 12 – 15 μm on occasion (see Figure 3), demonstrating that lipid-encapsulated DFB has the potential to remain stable at 37°C for a wide range of sizes relevant to medical imaging and therapeutic applications. That droplets this large existed after extrusion through a 1 μm-pore membrane may be due to some coalescence, but it is expected that this is primarily a result of the low perfluorocarbon surface tension. This, taken in conjunction with the high lipid concentrations used in this formulation and the lack of small bubbles upon acoustic energy provide evidence that the sub-micron content most likely consists of naturally-forming vesicles rather than DFB droplets.

The vaporization threshold for ADV agents varies widely in the literature, as there are many influencing test factors that modulate the pressure needed (e.g. ultrasound frequency, pulse length, duty cycle, ambient temperature).[15,17,31–35] The method used in this study to determine the threshold - by optical verification of individual droplets stationary near the bottom of the tube - differed from the approach of most studies to date (characterizing the mean echo amplitude returned from a bulk sample after vaporization)[17,18]. Additionally, several studies have shown that the acoustic pressure field in a microcellulose tube can differ greatly from the free-field hydrophone measurements and is a function of frequency, making direct comparisons across studies difficult.[16,35] However, a preliminary study by our group showed that under similar test conditions and threshold definitions, dodecafluoropentane droplets of the same size required as much as 40 – 50 % more pressure to induce vaporization.[27]

Microbubble Condensation Nanodroplets: Microbubble Size Prior to Condensation

To test our hypothesis that the size of resultant nanodroplets condensed from pre-formulated microbubbles correlates with the original microbubble populations, initial sizing was performed on prepared microbubbles at three lipid concentrations (Figure 4). In general, the

mode bubble size for each concentration was relatively similar, although for the 3 mg/mL formulation a much larger percentage of bubbles measuring greater than 1.5 μm in diameter resulted. This was not surprising as the higher lipid concentration may stabilize larger bubbles and skew the distribution somewhat.

Sub-micron Particle Analysis of Microbubble Condensation Nanodroplets

By assuming the number of moles is preserved between the liquid state and the gaseous state, a theoretical relationship can be developed from ideal gas laws that relates the size of the gas microbubbles to the size of the droplets that should be produced from microbubble condensation.[27] Sizing of resultant nanodroplets by the Malvern ZS demonstrated that the microbubble condensation method routinely produced peaks in the 200–300 nm range, which corresponds well with ideal gas law estimates of droplet sizes produced by the microbubble condensation method originating from bubbles in the 1– 2 μm range (as was the case with all microbubble preparations). While sub-micron particle sizing did not allow for information about concentration, all three lipid concentrations appeared to result in mode droplet sizes between 200 – 300 nm. A significant amount of variation across samples was observed with regard to the deviation from the mode size. Some samples were measured to have content below 100 nm, while others had only content greater than 200 nm (Figure 5) possibly reflecting some vesicle formation as lipid concentrations increased. We believe this variability may have resulted from inconsistencies in applied pressure and temperature at the time of condensation, but may also be partly due to formation of micelles and liposomes as a function of lipid concentration. This variability will be reduced as further refinements to the methodology are made.

Sizing of controls (i.e. prior to any microbubble generation) showed that the control 3 mg/mL formulation produced a peak near 100 nm at a low count rate (Figure 6) which may be attributed to naturally forming vesicles (as described previously). This peak was not present in any nanodroplet samples resulting from the 3 mg/mL lipid concentration, most likely as a result of the process of microbubble generation. Although the Malvern was not able to produce stable, consistent sizing results for the 0.75 mg/mL and 1.5 mg/mL samples, some content was present in the low nanometer range at lower count rates. These results suggest that the submicron sizings most likely represent viable, DFB-filled nanodroplets.

Micrometer-range Particle Sizing of Droplets Produced via Microbubble Condensation

The Malvern Nano ZS, which had an upper sizing threshold of 6 μm, showed the majority of the sample content to be in the nanometer range. However, to better characterize the content present in the micrometer range, the same samples previously presented in Figure 6 were also sized using an Accusizer 780A (Figure 7). The results showed that after microbubble condensation, some content as large as 2–4 μm was present in the sample, and the upper size limit seemed to increase with lipid concentration. The nature of this larger content is discussed later. These measurements help to support the success of the condensation method, as they show the mode particle size shifting towards the lower limit of sensitivity from the original bubble distribution near 1 μm. The distribution peaks of Figure 7 taken in conjunction with the sub-micron sizings of the same samples in Figure 6 suggest that the content in the micrometer-range represents a relatively small portion of the overall sample. We estimate that droplets larger than 600 nm typically only comprise between 1.5 – 4% of the overall sample by count while less than 1.5% of the total sample is between 1 μm and 6 μm. The concentration measured by the particle sizer decreased by approximately 2 orders of magnitude, presumably due to a reduction in particle size and a significant portion of the sample condensing to sizes below the sensitivity threshold, although secondary effects occurring during the generation (such as bubble breakage) could also be occurring.

Acoustic Droplet Vaporization of Decafluorobutane Microbubble Condensation Nanodroplets

Images with the focus positioned near the mid-plane of the microcellulose tube reflected droplet conversion captured immediately after vaporization, offering a true indication of the size distribution of microbubbles resulting from droplet vaporization as they passed through the optical focus due to buoyancy, although the rapid bubble rise toward the top of the tube resulted in some picture degradation (see Figure 8). Alternatively, images captured at the top of the tube (data not shown) when the bubbles had risen and collected (typically several seconds after the vaporization event) were useful for visualizing the 'bulk' group of microbubbles in-focus and taking more accurate measurements. It was noticed that measurements taken at the top of the tube reflected a somewhat skewed bubble size distribution when compared to the general sizes of bubbles observed during mid-plane videos and is likely due to the effect of larger bubbles at the apex of the tube obscuring smaller nearby bubbles. This was confirmed in multiple instances where smaller bubbles could be seen to be 'orbiting' much larger bubbles and fell out of view shortly afterward. While the mid-plane vaporization was useful for a 'snapshot' shortly after vaporization, the measurements taken at the top of the tube were more useful because the bubbles were stationary and the optical focus could be adjusted to capture a more complete distribution. Nonetheless, both approaches demonstrated the effect of lipid concentration on the number of bubbles produced from droplet vaporization.

As the droplets were not within the optical resolution of the experimental apparatus, it was necessary to measure the resulting bubbles as precisely as possible. Several studies have demonstrated the tendency of perfluorocarbon-filled microbubbles to uptake dissolved ambient gasses.[15,27,30] To reveal the influence of dissolved gas in the resulting microbubble population produced from vaporized nanodroplets, samples produced with a lipid concentration of 0.75 mg/mL were exposed to a 10 cycle pulse at 5 MHz (mechanical index of 1.7). Using the same sample throughout the test, bubbles resulting from droplet vaporization were measured at the top of the tube first in an un-degassed water bath (N = 239) followed by a degassed water bath (N = 228). The results show that simply degassing the water bath media reduced the maximum bubble size observed by 62% (from 32 μm to 12 μm). The mean and mode bubble sizes were also reduced by 36% and 20%, respectively.

Mid-plane observations in a degassed water bath revealed vaporization did produce a majority of bubbles in the 1 – 3 μm range independently of lipid concentration, although the number of bubbles produced increased dramatically when the lipid content was increased to 3 mg/mL (Figure 8). This may be because the higher lipid concentration produces better stabilization of bubbles through the condensation process and upon vaporization.

Table 1 lists the mean, mode, and maximum bubble size (rounded to the nearest 0.5 μm) observed for each lipid formulation at the two different pressures tested using bubbles measured from the top of the tube (N > 150 for each pressure). The mean and mode sizes were presumably higher than the true sample values due to reasons mentioned above. Minimum sizes were not included due to the fact that these could not be accurately compared across samples due to resolution limits, although in each lipid formulation the smallest bubble measured was near the optical resolution limit. In general, mean bubble size was similar across all samples, but mode bubble size decreased significantly as lipid concentration increased, indicating increased efficiency in preserving nanodroplets. This could also be observed in images of resulting bubbles, where higher lipid concentrations not only yielded more resulting bubbles per ultrasound pulse, but a proportionately higher distribution of small bubbles (see Figure 8).

Using the same 5 MHz frequency, it was observed that relatively similar distributions were observed at mechanical indices of 1.2 and 1.7, indicating the ultrasound pressure at MI = 1.2 was sufficient to induce vaporization across the same size ranges. However, a mechanical index of 1.7 did skew the population towards a larger proportion of smaller bubbles, implying the higher energy was more efficiently vaporizing nanodroplets (Table 1). The histograms of bubble sizes from each sample did not generally resemble original bubble sizing data well until the lipid concentration of 3 mg/mL was used. At 3 mg/mL, resulting bubble sizes displayed a strong peak in the 1 – 3 μm range with a precipitous drop-off toward higher sizes (Figure 9).

The extended ‘tail’ in Figure 9 is most likely due to the increased efficiency of vaporization for larger droplets – amplifying their presence proportionately. However, the presence of bubbles generally larger than those in the original agitated microbubbles requires further discussion. It was noticed that in several samples, especially those from higher lipid concentrations, some vaporizable droplets were present as large as 1–2 μm (< 1.5%), and on occasion could be observed as high as 3 – 4 μm. This indicates that the upper sizes shown in Figure 7 most likely represent droplet sizes rather than bubbles remaining in the sample (which were rarely, if ever, observed). By ideal gas law estimations, these droplets should result in bubbles on the order of 10 – 25 μm (see Table 1), explaining the presence of the larger vaporization-produced bubbles. These micron-sized droplets may be formed by larger microbubbles present after agitation, as the particle sizer does detect some bubbles as large as 25 – 30 μm in diameter, however, that bubbles larger than 15 μm typically comprise less than 0.09% of the overall population suggests that there may be other mechanisms at work. Because the samples were tested at high concentrations, it is possible that bubble fusion could result from the vaporization of droplets in very close proximity. If this were occurring, it would also have the effect of generally increasing the mode and mean bubble size compared to the original bubble population. It is also possible that the higher dissolved gas content of the samples due to room-air pressurization could lead to an increase in measured bubble size, although some of the dissolved gas would diffuse through the porous microcellulose tube into the degassed water bath before reaching the optical focus. This could be mediated in future studies by pressurization with low boiling-point, low solubility gasses. Alternately, secondary effects may be occurring during the condensation process. A brief experiment was performed to explore the interplay of pressure and temperature on microbubble condensation.

Influence of Secondary Effects on Microbubble Condensation

Agitated bubble samples were exposed to; a) cold only, or; b) pressurization with room-air only to determine effects on the bubble population (Figure 10). Results show that when exposed to reduced temperatures only, the bubble population did not change significantly. When exposed to pressure only, the bubble population begins shifting toward the sub-micron range (as shown previously), however, bubbles in the 20 – 30 μm size range begin to appear in higher proportion. This suggests that some degree of secondary effects – such as Ostwald ripening or bubble fusion – may be present during the pressurization process, which requires further investigation. These results also seem to show that pressure is the main driving force in the condensation procedure. Future studies will assess the resultant microbubble size as a function of the rate and degree of pressurization in order to ascertain whether these larger bubbles formed can be eliminated by refining of the process. In addition to secondary effects that result in the presence of larger bubbles, the effect that increased ambient pressure may have on causing a degree of microbubble dissolution prior to condensation will need to be studied further to optimize the technique.

Comparison of Methods

Direct comparison of the two methods employed is not appropriate in light of the different lipid and buffer formulations used. In the extrusion process, the aqueous solution was prepared in a way to lower the freezing point significantly in order to operate at temperatures where the bulk DFB solution would stay in the liquid phase. For the microbubble condensation method, the aqueous solution was prepared primarily to produce desired microbubble population characteristics. In these preliminary tests, the microbubble condensation method appeared to be a much simpler approach that could produce DFB droplets in large quantities. Although it is possible that an extrusion-based approach could be optimized in formulation and technique to produce comparable results, the low surface tension of perfluorocarbons and the high viscosity of the aqueous phase at the lower temperatures used present a significant challenge.

Conclusion

These preliminary results demonstrate that pressurization and temperature-induced condensation of pre-formed microbubbles may be both an effective and advantageous means of producing contrast agents for ADV applications compared to conventional extrusion and emulsion-based methods for some PFCs. The extent to which the method can be applied to PFCs of higher boiling points will require further investigation. The samples formed by microbubble condensation produced a high number of viable nanodroplets that could be vaporized at clinically feasible pressures, resulting in a distribution of contrast-providing microbubbles resembling the original microbubble sample. This method also may have advantages with regard to commercialization of ADV technology, as nanodroplets can be formed easily by adding a simple technique after traditional microbubble preparation.

These results highlight only two lipid formulations that can be used. Other lipid formulations should make this technology amenable to not only ultrasound imaging, but drug and gene delivery and therapy as well. The incorporation of 16:0 TAP in the lipid formulation used for microbubble condensation, which helped minimize aggregation and coalescence, is currently being pursued in our laboratories as a means of plasmid/gene delivery. In addition, the low concentrations of lipids (0.75 – 3.0 mg/mL) utilized to stabilize the DFB droplets makes these formulations more amenable to human use while also minimizing the possibility of toxicity or bioeffects.

This study represents our initial efforts to develop an extravascular ultrasound contrast agent based upon vaporizable nanodroplet technology. Results have demonstrated that ADV of submicron sized droplets can be induced *in vitro* with pressures available to clinical diagnostic ultrasound machines. Successful development of this exciting new agent may complement current efforts for developing tissue selective ultrasound contrast agents for both molecular imaging and therapy. Additional studies are ongoing to assess the level of stability, extent of extravasation, and selective tissue targeting of these agents.

Supplementary Material

Refer to Web version on PubMed Central for supplementary material.

Acknowledgments

This work was supported by NIH Grant # EB-011704. The authors appreciate the assistance of Dennis Given for extensive bubble sizing data. In addition, the authors acknowledge Professor Mark A. Borden in the Mechanical Engineering Department at the University of Colorado for insightful technical discussions regarding microbubble pressurization. Paul Sheeran acknowledges the generous support of the National Science Foundation as the recipient of a graduate fellowship.

References

1. [accessed April 4, 2011] Lantheus Medical Imaging. http://www.definityimaging.com/main.html
2. Wilson SR, Burns PN. Radiology. 2010; 257:24–39. [PubMed: 20851938]
3. ten Kate GL, Sijbrands EJ, Valkema R, ten Cate FJ, Feinstein SB, van der Steen AF, Daemen MJ, Schinkel AF. J Nucl Cardiol. 2010; 17:897–912. [PubMed: 20552308]
4. Stieger SM, Dayton PA, Borden MA, Caskey CF, Griffey SM, Wisner ER, Ferrara KW. Contrast Media Mol Imaging. 2008; 3:9–18. [PubMed: 18335479]
5. Gessner R, Dayton PA. Mol Imaging. 2010; 9:117–127. [PubMed: 20487678]
6. Anderson CR, Hu X, Zhang H, Tlaxca J, Decleves AE, Houghtaling R, Sharma K, Lawrence M, Ferrara KW, Rychak JJ. Invest Radiol. 2011; 46:215–224. [PubMed: 21343825]
7. Hobbs SK, Monsky WL, Yuan F, Roberts WG, Griffith L, Torchilin VP, Jain RK. Proc Natl Acad Sci U S A. 1998; 95:4607–4612. [PubMed: 9539785]
8. Ng, KY.; Matsunaga, TO. Drug Delivery: Principles and Applications. Wang, B.; Siahaan, T.; Soltero, R., editors. New Jersey: John Wiley & Sons, Inc.; 2005. p. 245-278.
9. Landmark KE, Johansen PW, Johnson JA, Johansen B, Uran S, Skotland T. Ultrasound Med Biol. 2008; 34:494–501. [PubMed: 18096304]
10. Mullin L, Gessner R, Kwan J, Kaya M, Borden MA, Dayton PA. Contrast Media Mol Imaging. 2011 In Press.
11. Zhang M, Fabiilli ML, Haworth KJ, Fowlkes JB, Kripfgans OD, Roberts WW, Ives KA, Carson PL. Ultrasound Med Biol. 2010; 36:1691–1703. [PubMed: 20800939]
12. Zhang P, Porter T. Ultrasound Med Biol. 2010; 36:1856–1866. [PubMed: 20888685]
13. Schad KC, Hynynen K. Phys Med Biol. 2010; 55:4933–4947. [PubMed: 20693614]
14. Rapoport NY, Kennedy AM, Shea JE, Scaife CL, Nam KH. J Control Release. 2009; 138:268–276. [PubMed: 19477208]
15. Kripfgans OD, Fowlkes JB, Miller DL, Eldevik OP, Carson PL. Ultrasound Med Biol. 2000; 26:1177–1189. [PubMed: 11053753]
16. Kripfgans OD, Fabiilli ML, Carson PL, Fowlkes JB. J Acoust Soc Am. 2004; 116:272–281. [PubMed: 15295987]
17. Fabiilli ML, Haworth KJ, Fakhri NH, Kripfgans OD, Carson PL, Fowlkes JB. Ultrasonics, Ferroelectrics and Frequency Control, IEEE Transactions. 2009; 56:1006–1017. on.
18. Kripfgans OD, Fowlkes JB, Woydt M, Eldevik OP, Carson PL. Ultrasonics, Ferroelectrics and Frequency Control, IEEE Transactions. 2002; 49:726–738. on.
19. Kripfgans OD, Orifici CM, Carson PL, Ives KA, Eldevik OP, Fowlkes JB. Ultrasonics, Ferroelectrics and Frequency Control, IEEE Transactions. 2005; 52:1101–1110. on.
20. Kawabata K, Sugita N, Yoshikawa H, Azuma T, Umemura S. Jpn. J. Appl. Phys. Part 1 - Regul. Pap. Short Notes Rev. Pap. 2005; 44:4548–4552.
21. Couture O, Bevan PD, Cherin E, Cheung K, Burns PN, Foster FS. Ultrasound in Medicine & Biology. 2006; 32:1247–1255. [PubMed: 16875958]
22. Couture O, Bevan PD, Cherin E, Cheung K, Burns PN, Foster FS. Ultrasound in Medicine & Biology. 2006; 32:73–82. [PubMed: 16364799]
23. Antoine C. Comptes Rendus. 1888; 107:681–684.
24. Borden MA, Pu G, Runner GJ, Longo ML. Colloids Surf B Biointerfaces. 2004; 35:209–223. [PubMed: 15261034]
25. Alexandridis P, Athanassiou V, Fukuda S, Hatton TA. Langmuir. 1994; 10:2604–2612.
26. Lide, DR. Handbook of Chemistry and Physics, 90th Edition (Internet Version 2011). Florida: CRC Press/Taylor and Francis; 2011.
27. Sheeran PS, Wong VP, Luois S, McFarland RJ, Ross WD, Feingold S, Matsunaga TO, Dayton PA. Ultrasound in Medicine & Biology. 2011 In Press.
28. Unger, EC.; Fritz, TF.; Matsunaga, TO.; Ramaswami, R.; Yellowhair, D.; Wu, G. U.S. Patent. No. 5,469,854. 1995.
29. Evans DR, Parsons DF, Craig VSJ. Langmuir. 2006; 22:9538–9545. [PubMed: 17073477]

30. Kwan JJ, Borden MA. Langmuir. 2010; 26:6542–6548. [PubMed: 20067292]
31. Giesecke T, Hynynen K. Ultrasound Med Biol. 2003; 29:1359–1365. [PubMed: 14553814]
32. Lo AH, Kripfgans OD, Carson PL, Rothman ED, Fowlkes JB. IEEE Trans Ultrason Ferroelectr Freq Control. 2007; 54:933–946. [PubMed: 17523558]
33. Schad KC, Hynynen K. Phys Med Biol. 2010; 55:4933–4947. [PubMed: 20693614]
34. Zhang P, Porter T. Ultrasound Med Biol. 2010; 36:1856–1866. [PubMed: 20888685]
35. Qin S, Kruse DE, Ferrara KW. Ultrasound Med Biol. 2008; 34:1014–1020. [PubMed: 18395962]

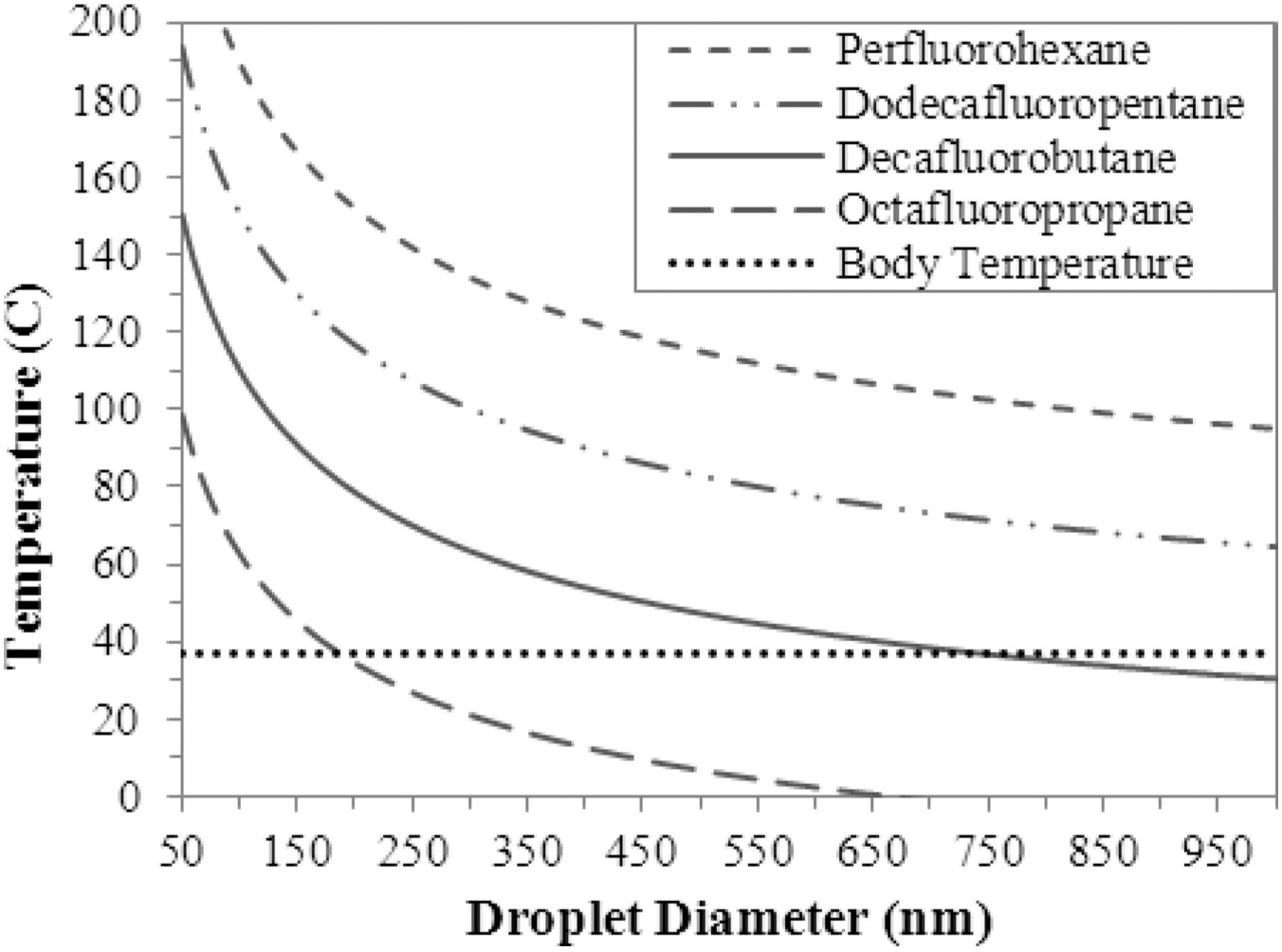

Figure 1.

Estimations based on the Antoine equation demonstrate that DFB is a promising compound for developing metastable nanoparticles due to its low vaporization energy for particles in the 100 – 750 nm range compared to other PFCs typically studied as phase-change contrast agents. Curves that rise above body temperature indicate potential for the encapsulated PFC droplets to remain stable for the specified sizes due to the increased surface tension effects. Calculations were performed using atmospheric pressure and a surface tension of 51 mN/m for all compounds. This surface tension value was chosen based on lipid formulations previously used by our group, and because it is near the upper limits that have been reported in the literature[24,25] for lipid or polymer encapsulation.

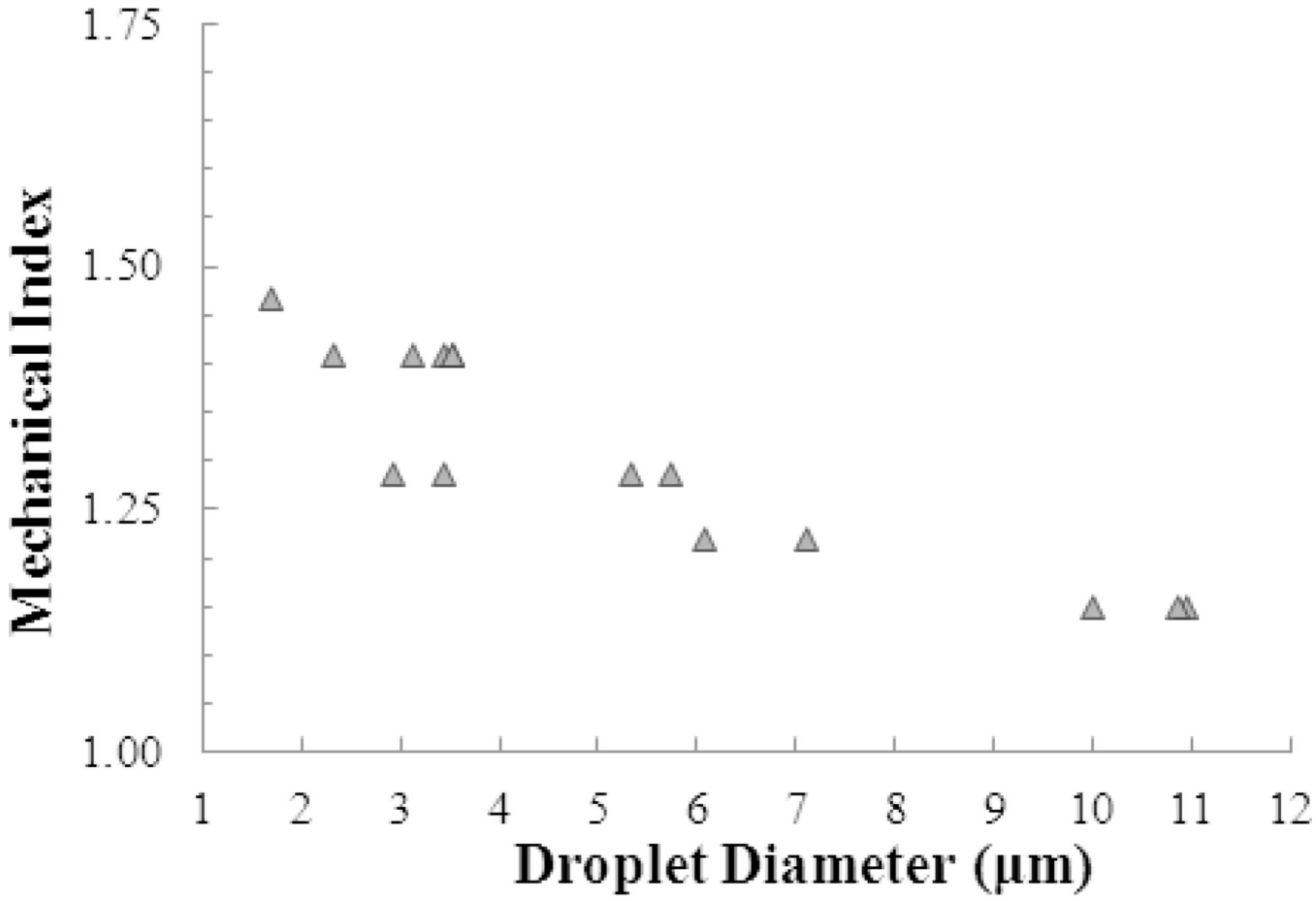

Figure 2.
DFB droplets with diameters in the low micron range were seen to vaporize as an inverse function of initial diameter (N = 15). Droplets near the optical resolution limit of the experimental setup could be vaporized with brief 2 μs pulses at mechanical indices well-below the current clinical limit of 1.9 for diagnostic ultrasound imaging.

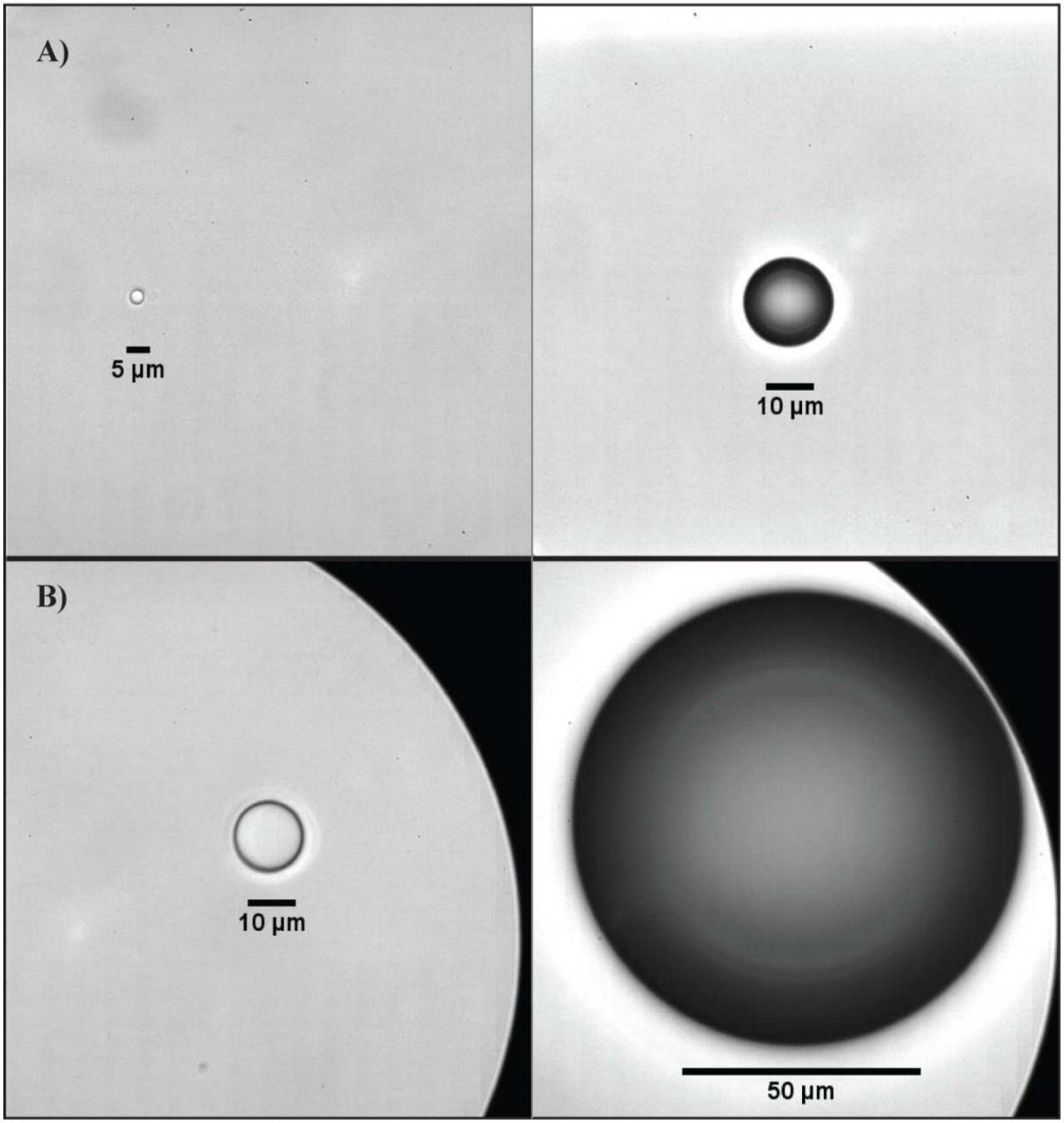

Figure 3.
Micron-sized DFB droplets produced by membrane extrusion were stable at 37°C and could be subsequently vaporized by ultrasonic energy. The extrusion method produced a highly varying size distribution of viable droplets, including (a) droplets near the optical resolution of the system, and (b) some larger than 10 μm in diameter. The resulting increase in size after vaporization was close to that predicted by ideal gas laws (approximately 5 to 6 times the original droplet diameter).

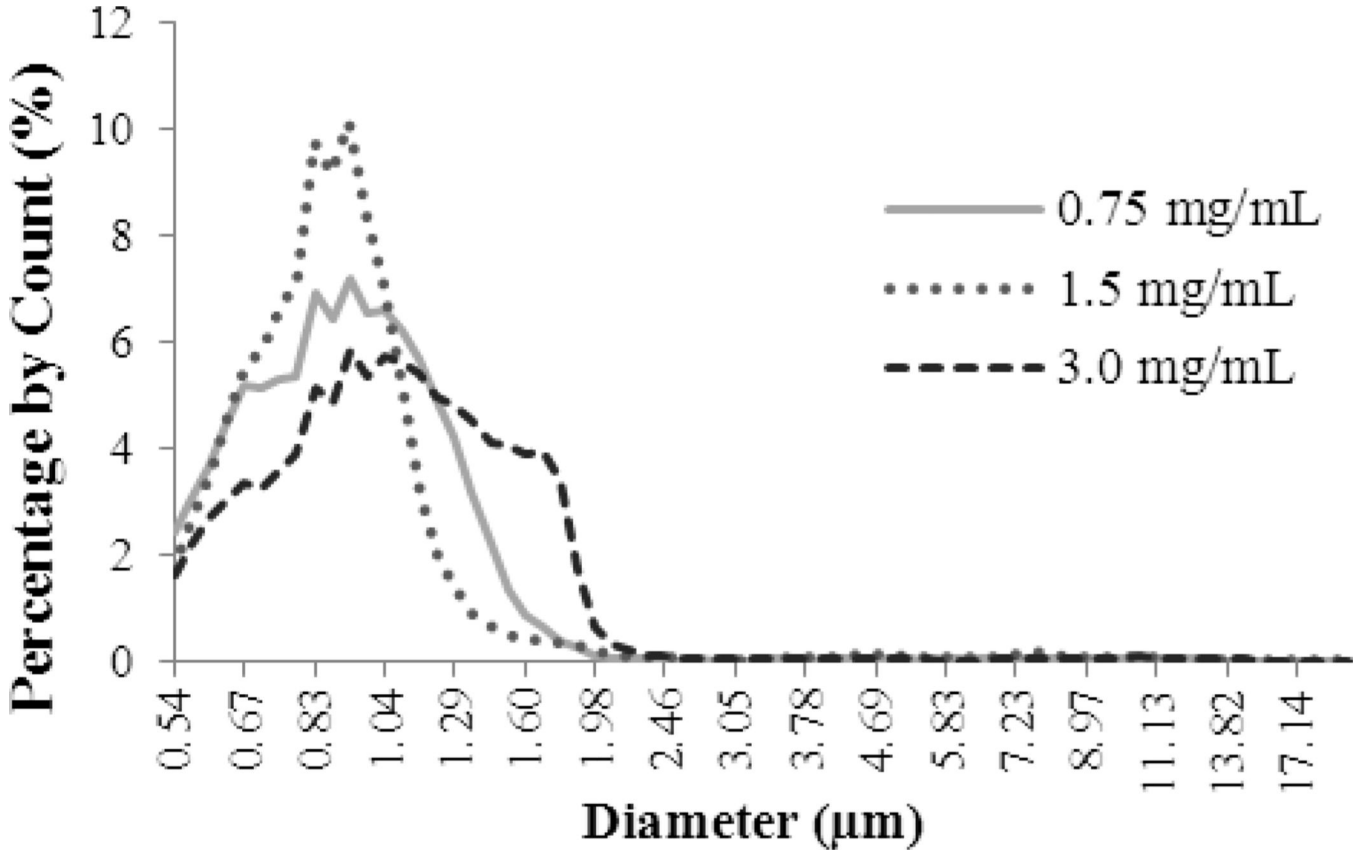

Figure 4.

Representative bubble populations prior to microbubble condensation. Mean bubble size for each lipid in order of increasing lipid concentration was 1.03 μm, 1.01 μm, and 1.20 μm, while mode bubble size was 0.93 μm for all three. Concentrations in particles/mL were 4.8×10^9, 3.1×10^9, and 9.9×10^9, respectively.

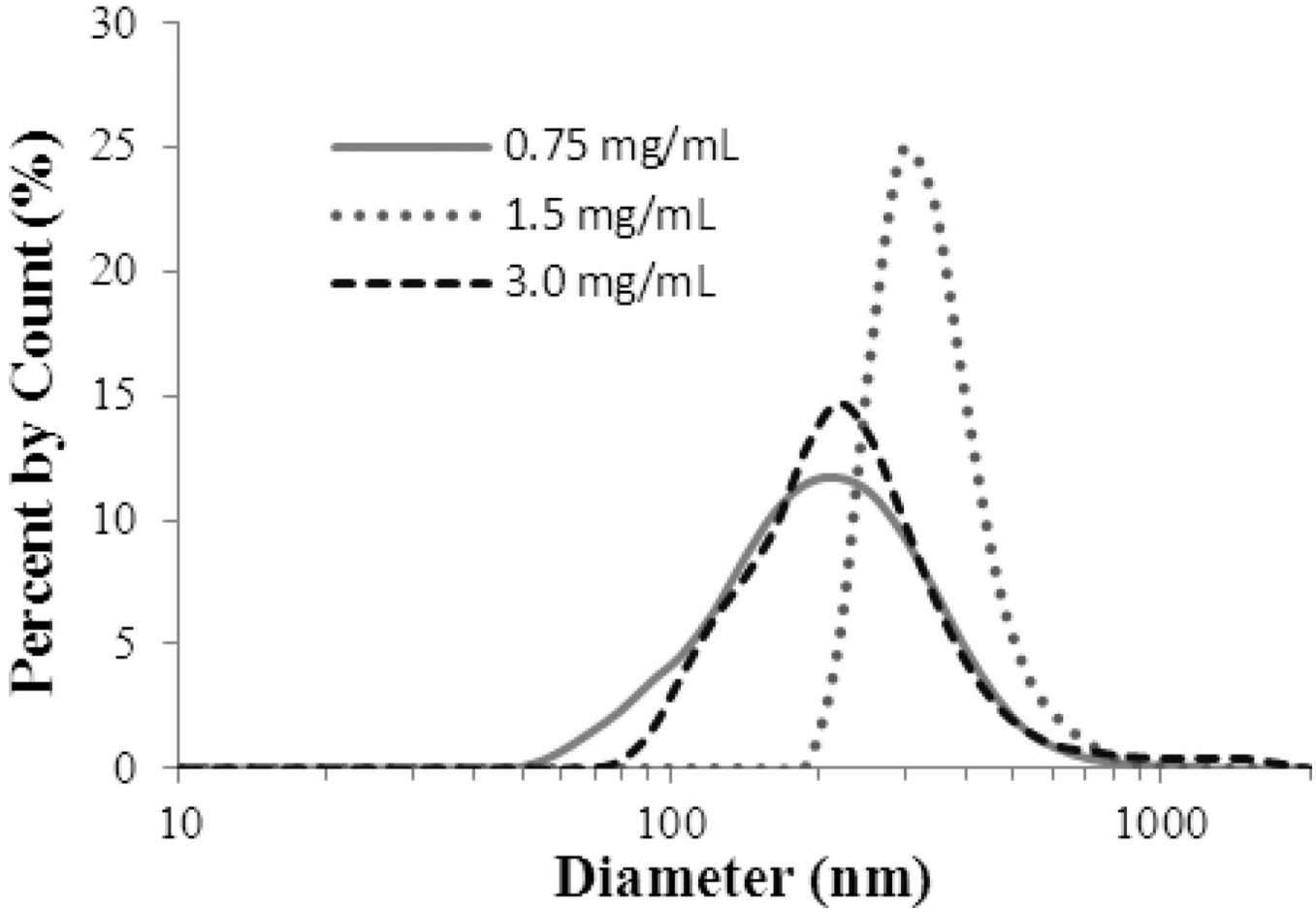

Figure 5.
Example of sub-micron particle sizing of nanodroplets produced by the microbubble condensation method. Peak sizes of 200–300 nm resulted which appeared to be independent of lipid concentration. Mean droplet size for each curve in order of increasing lipid concentration was 229 ± 120 nm, 345 ± 97 nm, and 325 ± 268 nm, respectively, while mode droplet size was 220 nm, 295 nm, and 255 nm.

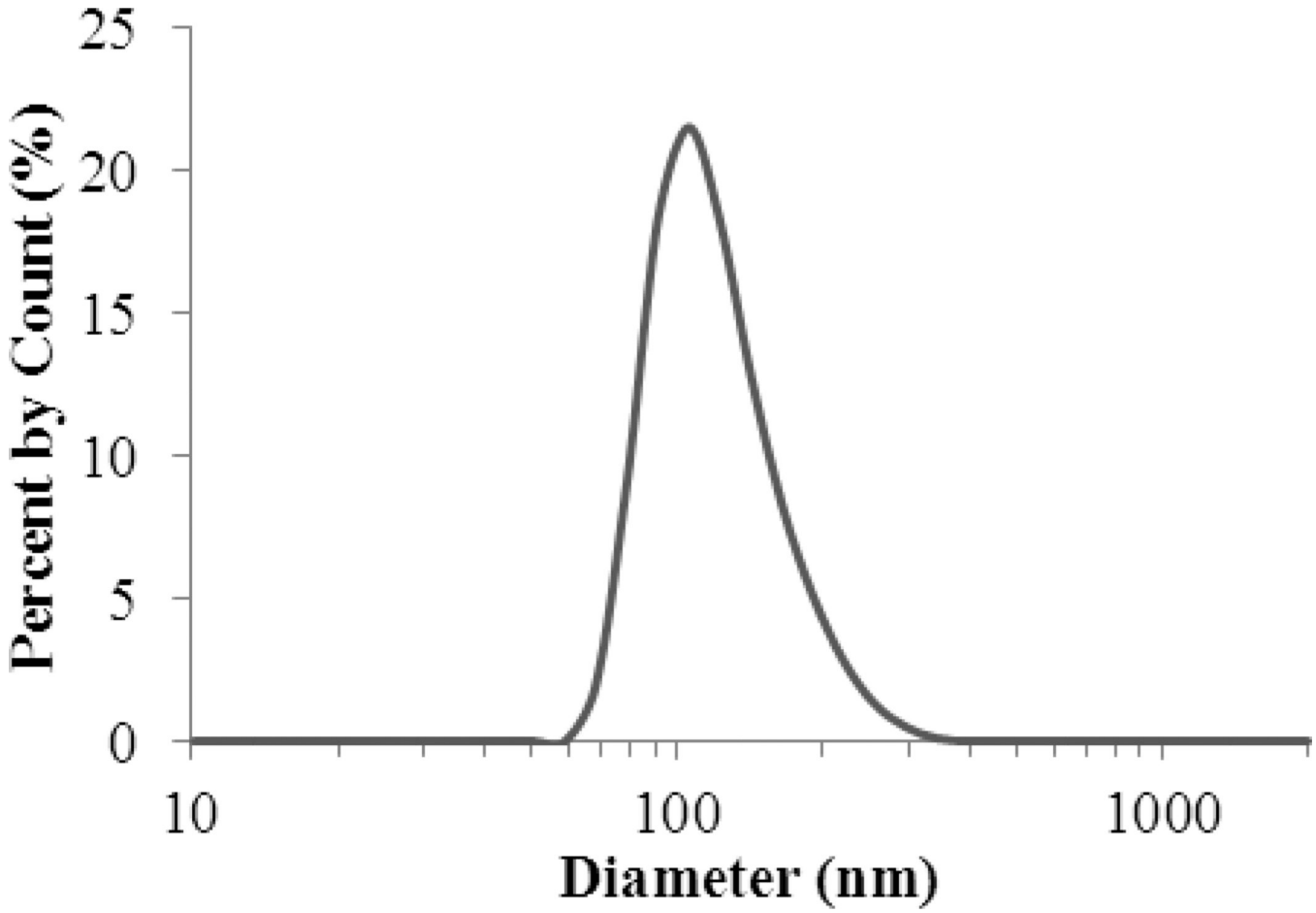

Figure 6.
Lipid control solution sub-micron sizing. A peak at 105 nm with a low count rate was detected for the 3 mg/mL lipid solution, which did not appear in droplet samples at the same lipid concentration.

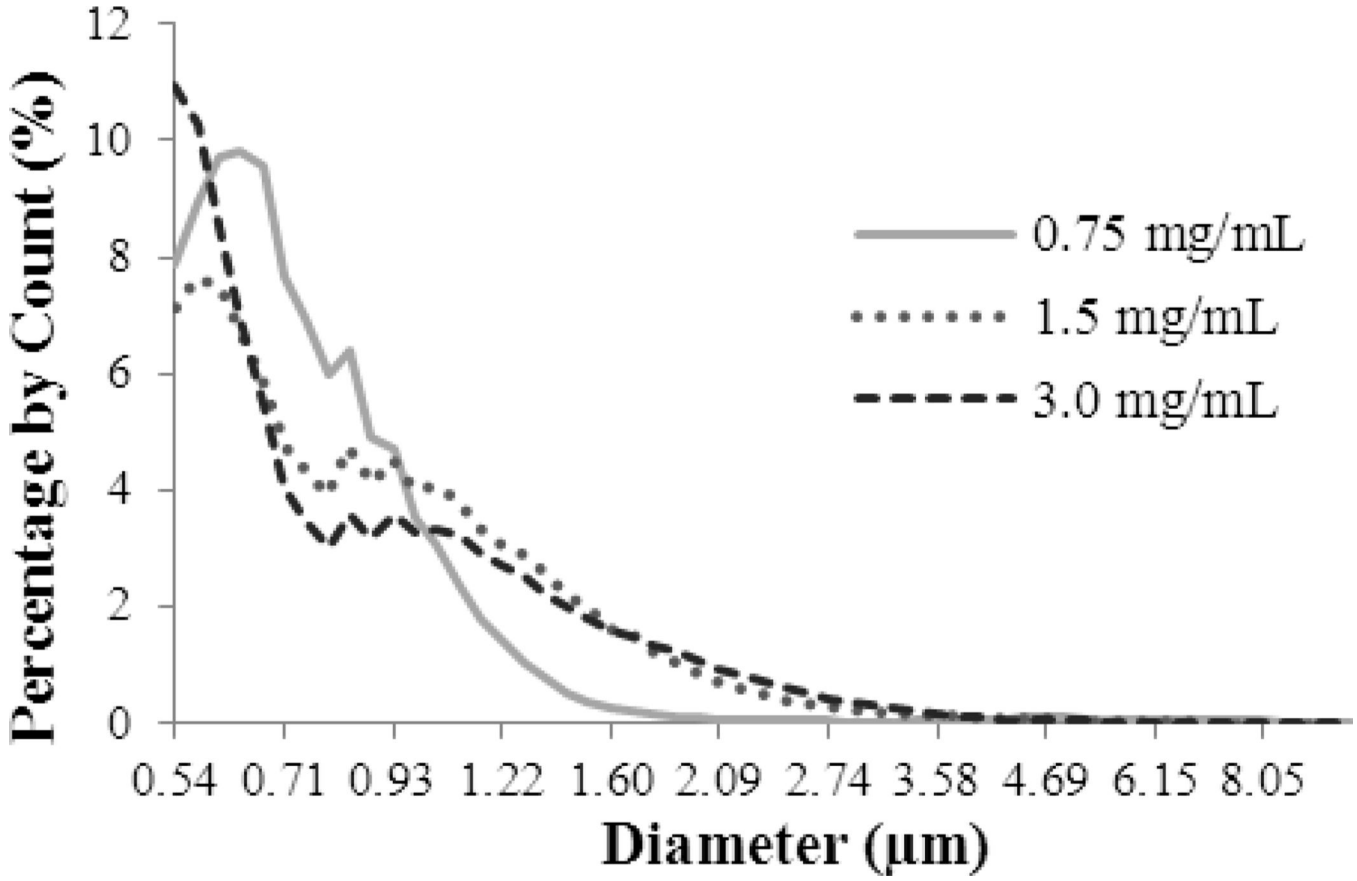

Figure 7.

Condensation of original microbubble samples shows a shift of mode size into the sub-micron range, as captured by an Accusizer 780A. For each lipid concentration, the resulting mode size (0.64 µm, 0.57 µm, and 0.54 µm in order of increasing concentration) was near the lower sensitivity of the machine (0.54 µm), indicating the sample is likely better represented by the results of the sub-micron particle sizing (Figure 6). The data corresponds well with measured resultant microbubble size after ADV as shown in Table 1. Concentrations in particles/mL were 1.2×10^7, 2.4×10^7, and 8.4×10^7, respectively.

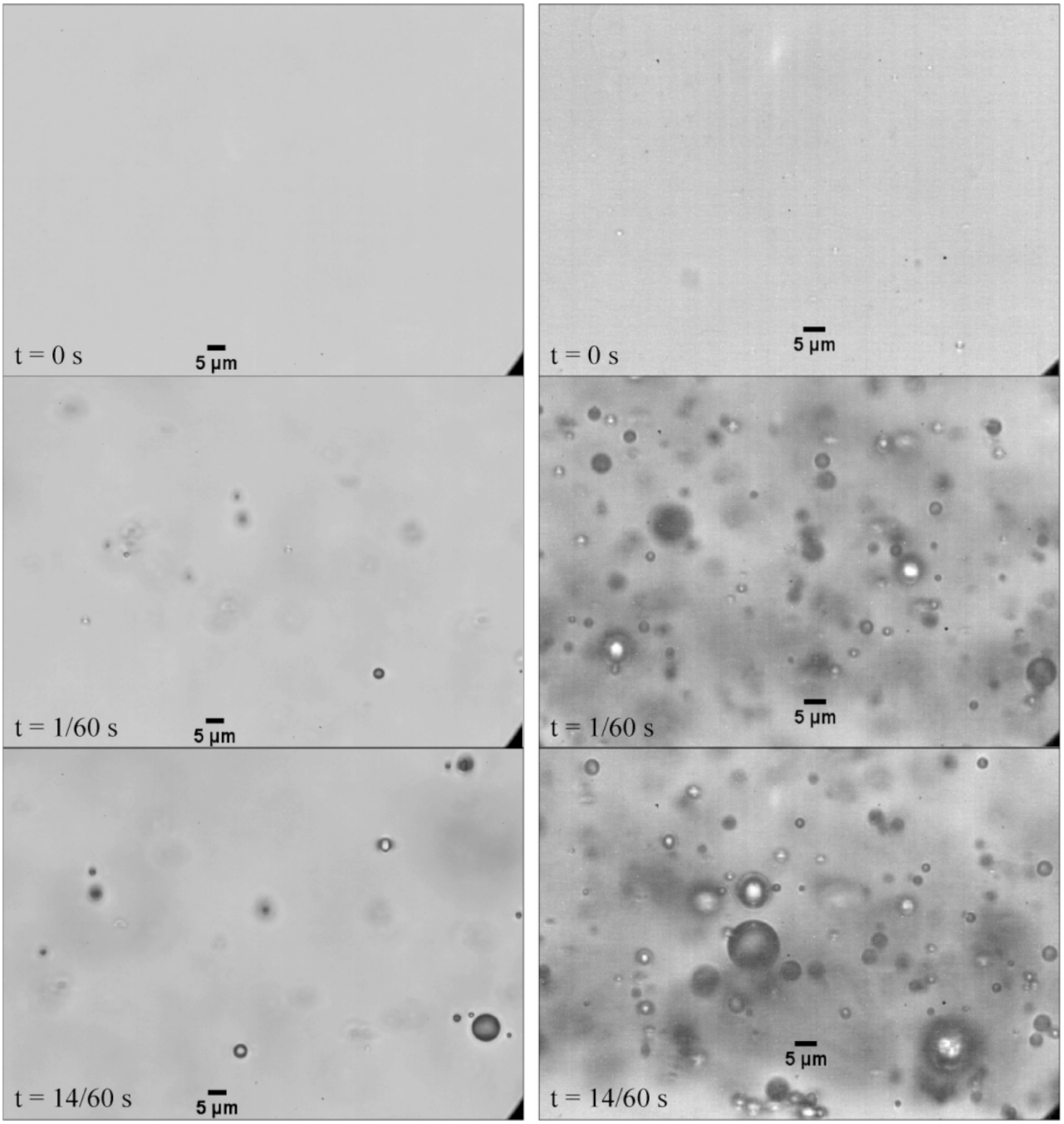

Figure 8.

Mid-plane droplet vaporization revealed microbubble sizes occurring predominantly in the 1 –3 μm range, with an increasing number of bubbles produced as lipid concentration increased. Vaporization was induced with a 10 cycle pulse at 5 MHz with a mechanical index of 1.7. Left: 0.75 mg/mL lipid concentration. Right: 3.0 mg/mL lipid concentration.

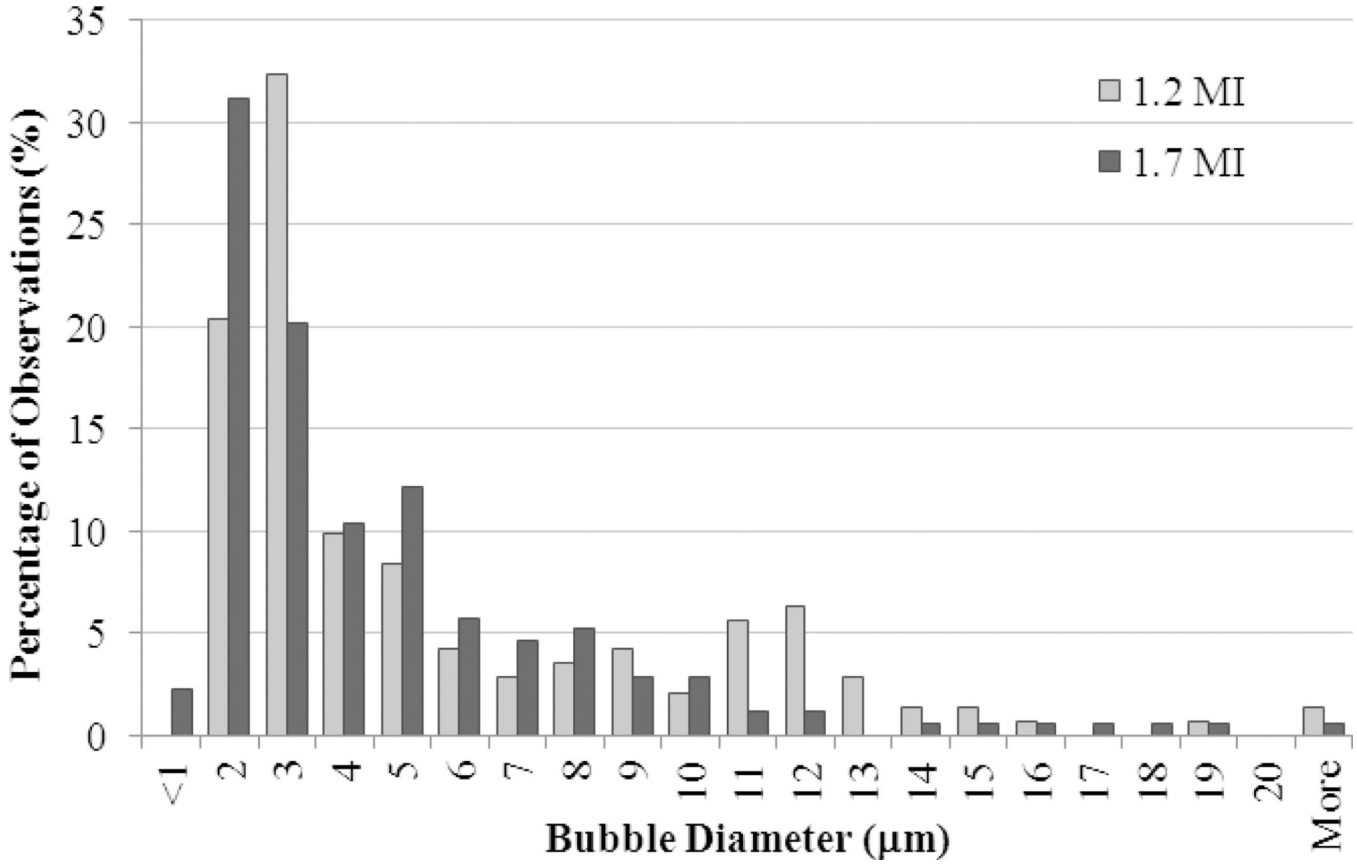

Figure 9.

Resulting bubble diameter as a function of increasing acoustic pressure for samples originating from 3 mg/mL lipid solutions measured from bubbles collected at the top of the microcellulose tube. Sizing profiles resemble original microbubble sizing profiles, indicating successful generation and vaporization of condensed microbubbles. Mechanical indices of 1.2 and 1.7 result in similar bubble distributions, however, it is noted the higher pressure produces a greater proportion of bubbles in the 1 – 2 μm range.

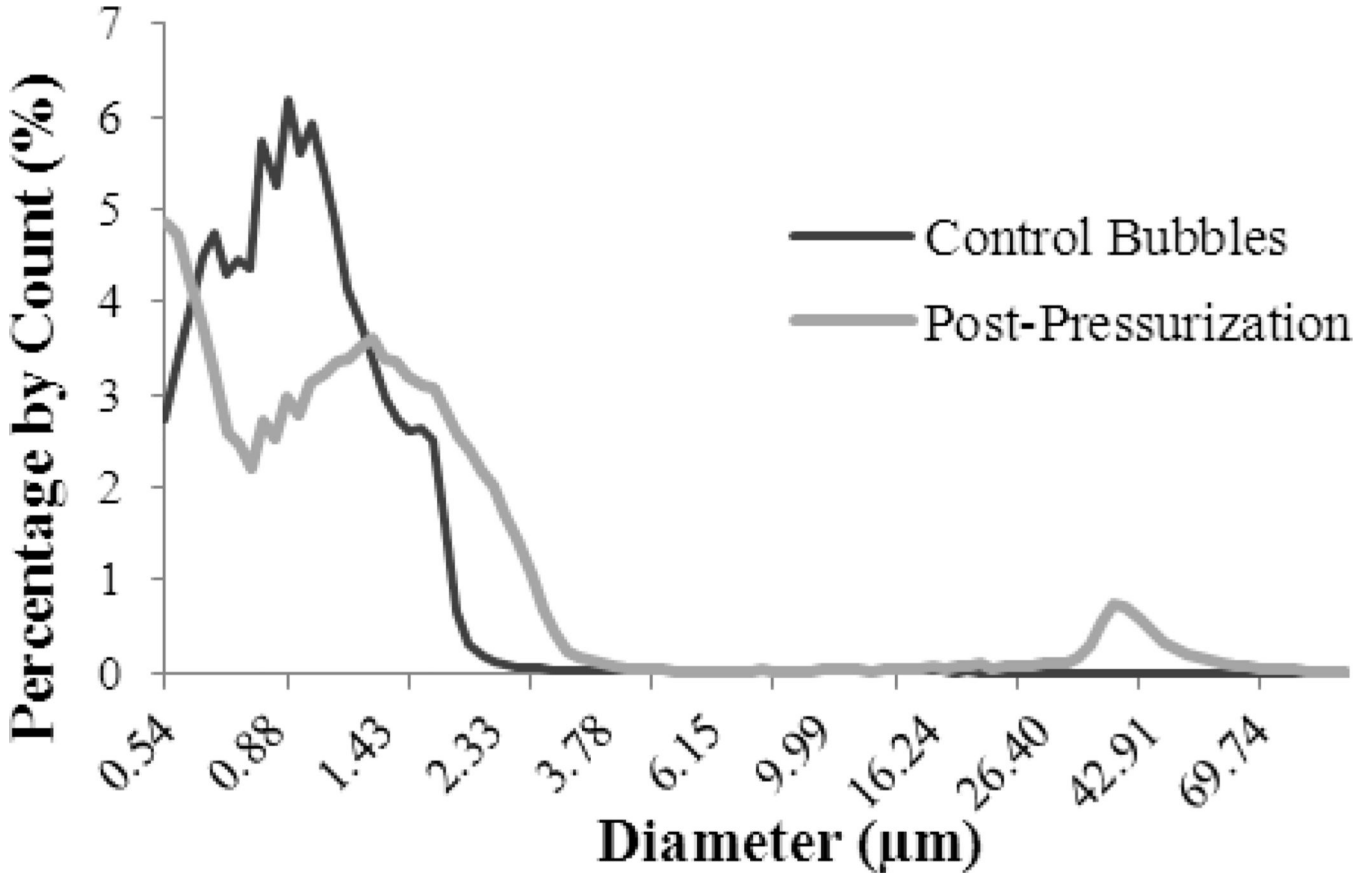

Figure 10.

Agitated microbubbles (3 mg/mL lipid concentration) exposed to room-air pressure only show transition of mode size into the sub-micron range, although the presence of bubbles in the 20–30 micron size range increases in proportion, suggesting secondary effects may be occurring to some degree. Concentrations in particles/mL for the control bubbles and pressurized sample were 4.8×10^{9} and 2.5×10^{8}, respectively.

Table 1

Resulting Bubble Sizes

	Mean (μm)		Mode (μm)		Maximum (μm)	
	MI = 1.2	**MI = 1.7**	**MI = 1.2**	**MI = 1.7**	**MI = 1.2**	**MI = 1.7**
0.75 mg/mL	5.5 ± 2.5	5.0 ± 2.5	6.0	6.0	12.0	12.0
1.5 mg/mL	5.5 ± 4.5	6.5 ± 4.0	5.5	4.0	20.0	19.0
3.0 mg/mL	5.0 ± 4.5	4.0 ± 4.0	2.0	1.5	26.0	25.5

Langmuir. Author manuscript; available in PMC 2012 September 6.